Mon. Not. R. Astron. Soc. **424,** 1105–1112 (2012) doi:10.1111/j.1365-2966.2012.21284.x

Cores in warm dark matter haloes: a Catch 22 problem

Andrea V. Macciò,[1⋆] Sinziana Paduroiu,[2] Donnino Anderhalden,[3] Aurel Schneider[3] and Ben Moore[3]

[1]*Max-Planck-Institute for Astronomy, Königstuhl 17, D-69117 Heidelberg, Germany*
[2]*Geneva Observatory, University of Geneva, CH-1290 Sauverny, Switzerland*
[3]*Institute for Theoretical Physics, University of Zürich, CH-8057 Zürich, Switzerland*

Accepted 2012 May 10. Received 2012 April 24; in original form 2012 February 11

ABSTRACT

The free streaming of warm dark matter particles dampens the fluctuation spectrum, flattens the mass function of haloes and sets a fine-grained phase density limit for dark matter structures. The phase-space density limit is expected to imprint a constant-density core at the halo centre in contrast to what happens for cold dark matter. We explore these effects using high-resolution simulations of structure formation in different warm dark matter scenarios. We find that the size of the core we obtain in simulated haloes is in good agreement with theoretical expectations based on Liouville's theorem. However, our simulations show that in order to create a significant core ($r_c \sim 1$ kpc) in a dwarf galaxy ($M \sim 10^{10}\,M_\odot$), a thermal candidate with mass as low as 0.1 keV is required. This would fully prevent the formation of the dwarf galaxy in the first place. For candidates satisfying large-scale structure constraints (m_ν larger than ≈1–2 keV), the expected size of the core is of the order of 10 (20) pc for a dark matter halo with a mass of 10^{10} (10^8) $M_\odot$. We conclude that 'standard' warm dark matter is not a viable solution for explaining the presence of cored density profiles in low-mass galaxies.

Key words: galaxies: haloes – dark matter.

1 INTRODUCTION

The formation of structure in the universe is driven by the mysterious dark matter component whose nature is still unknown. Over the last decades, the hierarchical cold dark matter (CDM) model has become the standard description for the formation of cosmic structures. It is in excellent agreement with recent observations, such as measurements of the cosmic microwave background and large-scale surveys (Tegmark et al. 2006; Komatsu et al. 2011). However, there are a number of inconsistencies on subgalactic scales that arise within the CDM scenario. First, the amount of substructure in Milky Way (MW) sized haloes is overpredicted by roughly one order of magnitude (Klypin et al. 1999; Moore et al. 1999). Secondly, the central densities of CDM haloes in simulations show a cuspy behaviour (Flores & Primack 1994; Moore 1994; Diemand et al. 2005; Macciò et al. 2007; Springel et al. 2008), whereas the density profiles inferred from galaxy rotation curves point to a core-like structure (e.g. Kuzio de Naray, McGaugh & Mihos 1999; de Blok et al. 2001; Oh et al. 2011). Furthermore, recent studies (Tikhonov et al. 2009; Zavala et al. 2009; Peebles & Nusser 2010) re-emphasized that also the population of dwarf galaxies within voids is in strong contradiction with CDM predictions.

One possible solution to these issues is that the dark matter particle is a thermal relic with a mass of the order of 1 keV. The most prominent representatives of such warm dark matter (WDM) candidates are the sterile neutrino and the gravitino (Abazajian & Koushiappas 2006; Boyarsky, Ruchayskiy & Shaposhnikov 2009a), whose presence is also motivated by particle theory (e.g. Dodelson & Widrow 1994; Takayama & Yamaguchi 2000; Buchmüller et al. 2007).

Non-zero thermal velocities for WDM particles lead to a strong suppression of the linear matter power spectrum on galactic and subgalactic scales (Bond, Efstathiou & Silk 1980; Pagels & Primack 1982; Dodelson & Widrow 1994; Hogan & Dalcanton 2000; Zentner & Bullock 2003; Viel et al. 2005; Abazajian 2006), and erase all primordial density perturbations smaller than their free-streaming scale λ_{fs}. Below this scale no structure is expected to form, at least not in the usual bottom-up scenario. However, the effective suppression of halo formation already happens well above λ_{fs} and is entirely described by the WDM particle mass (see Smith & Markovic 2011, and references therein).

Recent observational constraints coming from X-ray background measurements and Lyα forest analysis set the allowed mass interval

⋆E-mail: maccio@mpia.de

roughly between 2 and 50 keV (e.g. Viel et al. 2005; Abazajian & Koushiappas 2006; Seljak et al. 2006; Boyarsky et al. 2009b; Boyarsky, Ruchayskiy & Iakubovskyi 2009c).[1] As a complementary study, Macciò & Fontanot (2010, see also Polisensky & Ricotti 2011) compared the subhalo abundance of an MW-like object in different numerical WDM realizations with observed satellite galaxies reported by the Sloan Digital Sky Survey data and set a lower bound for a thermalized particle of $m_{\rm WDM} \gtrsim 2$ keV.

Another important characteristic of a WDM scenario is the possibility to *naturally* obtain cored matter density profiles. According to Liouville's theorem for collisionless systems, the fine-grained phase-space density of the cosmic fluid stays constant through cosmic history. In WDM the dark matter fluid is described by a Fermi–Dirac distribution, whose absolute value is fixed at the time of decoupling when the fluid becomes collisionless. Structure formation then happens through a complex process of distortion and folding of the phase-space sheet. Since it is not possible to measure this fine-grained phase-space density in simulations, one usually defines a coarse-grained or pseudo-phase-space density (e.g. Taylor & Navarro 2001)

$$Q \equiv \frac{\rho}{\sigma^3}, \tag{1}$$

where ρ is the mean density and σ is the one-dimensional velocity dispersion within some small patch of the simulation.[2] The quantity Q corresponds to an average density of a small (but not microscopic) phase-space volume and is not constant anymore. However, because of the way the phase-space sheet is distorted, the value of Q in most of the cases can only decrease during structure formation and will not exceed its initial value set at decoupling (Dalcanton & Hogan 2001, see however Boyarsky et al. 2009c for a thorough discussion of the meaning of Q and its evolution with time).

This upper limit for Q also holds for the local pseudo-phase-space density within virialized haloes at redshift 0 and has a direct consequence on the density profile in real space. Since the velocity dispersion does not grow in the inner part of a halo, the real-space density profile must become constant with a core size depending on the specific WDM model (Tremaine & Gunn 1979).

Due to this effect of core formation, the WDM scenario has been suggested as a solution to the long-standing core–cusp problem of dwarf galaxies. In fact, observational measurements favour cored dark matter profiles in low surface brightness galaxies within the Local Group (Kuzio de Naray & Kaufmann 2011; Salucci et al. 2012). However, previous theoretical/analytical studies (e.g. de Vega, Salucci & Sanchez 2010) argue that the cores produced by WDM might be too small to explain the observations. For example, Bode, Ostriker & Turok (2001) argued that the principal effect of the thermal motion in the WDM scenario is to give the particle angular momentum, producing a centrifugal barrier keeping the particle away from $r = 0$; only for radii inside this barrier is the structure of the halo significantly altered with respect to a pure CDM halo. Assuming a flat rotation curve for the halo and spherical collapse, they estimated that for warm particles with masses larger than 1 keV, thermal velocities are not able to modify the structure of haloes on scales of a kiloparsec or above.

More recently, Villaescusa-Navarro & Dalal (2011) have employed the spherical collapse model to study the formation of haloes in WDM cosmologies. They found that the core sizes, for allowed WDM temperatures ($\sim$1 keV), are typically very small, of the order of 10^{-3} of the halo virial radius at the time of formation, and considerably smaller following formation. They concluded that for realistic WDM models the core radii of haloes observed at $z = 0$ are generically expected to be far smaller than the core sizes measured in local low surface brightness galaxies. One of the aims of our work is to test these previous analytical results using self-consistent cosmological N-body simulations of halo formation in a WDM universe.

Numerical N-body simulations have been used to better understand the properties of virialized objects in the WDM scenarios (e.g. Bode et al. 2001; Knebe et al. 2003; Wang & White 2007; Tikhonov et al. 2009; Zavala et al. 2009; Schneider et al. 2011). High-resolution simulations of single objects have studied the suppression of the galactic satellite formation due to free streaming (e.g. Colín, Avila-Reese & Valenzuela 2000; Götz & Sommer-Larsen 2002; Knebe et al. 2008; Macciò & Fontanot 2010), in order to reconcile the observed dwarf galaxy abundance with the prediction from dark matter based theories. More recently, Colín, Valenzuela & Avila-Reese (2008) used N-body simulations to study the effects of primordial (thermal) velocities on the inner structure of dark matter haloes, with particular attention on the formation of a possible central density core. They used thermal velocities of the order of 0.1 and 0.3 km s^{-1}, without linking them to any particular WDM model, since the aim of their work was to explore the general effect of relic velocities of the dark matter structure. Unfortunately, their combination of resolution and choice for relic velocities was not sufficient to directly test simulation results against core radii predicted by phase-space constraints.

In this work, we want to extend and improve on these previous studies. We will use high-resolution N-body simulations to explore the sizes of density cores in WDM and their dependence on the WDM candidate mass.[3] We will explore several models for WDM ranging from 2 to 0.05 keV. We will consider separately the effects of a WDM candidate on the power spectrum and on the relic velocities, trying to disentangle the various consequences of these two different components. Our higher numerical resolution will allow us to directly see the formation of a density core, with a size well above the numerical resolution for the warmer candidates. We will then revise the theoretical arguments for the formation of cored profiles in WDM and perform a direct comparison between the core sizes in our simulations and the ones predicted from phase-space constraints.

This paper is structured as follows. In Section 2, we discuss the set-up of our simulations and the way we implement thermal velocities. Section 3 is dedicated to the presentation of our results in terms of the phase-space limit and its influence on the density

[1] In some of these analyses, the WDM particle is assumed to be a resonantly produced sterile neutrino (Shi & Fuller 1999). We have converted these mass limits into limits for a fully thermalized particle, such as the gravitino, using the formula provided by Viel et al. (2005).

[2] In the context of a non-singular isothermal sphere, the quantity Q is directly proportional to the maximum phase-space density and can be described, as in Tremaine & Gunn (1979), as giving the maximum coarse-grained phase-space density. In a more general context, applicable to simulations, the velocity distribution of the particles is not Maxwellian and hence Q does not really trace the coarse-grained phase-space density and hence we will refer to it as *a pseudo-phase-space density*.

[3] In the present work, we only considered a very simple WDM model; it is worth commenting that there are more complex and physically motivated models discussed in the literature (e.g. warm+cold dark matter: Boyarsky et al. 2009d; Macciò et al. 2012b; or composite dark matter: Khlopov 2006; Khlopov & Kouvaris 2008).

profile of dark matter haloes. A conclusion and summary of our work is finally given in Section 3.

2 SIMULATIONS

Numerical simulations have been carried out using PKDGRAV, a treecode written by Joachim Stadel and Thomas Quinn (Stadel 2001). The initial conditions are generated with the GRAFIC2 package (Bertschinger 2001). All simulations start at redshift $z_i = 99$ in order to ensure a proper treatment of the non-linear growth of cosmic structures.

The cosmological parameters are set as follows: $\Omega_\Lambda = 0.727$, $\Omega_m = 0.273$, $\Omega_b = 0.044$, $h = 0.7$ and $\sigma_8 = 0.8$, and are in good agreement with the recent *Wilkinson Microwave Anisotropy Probe* mission results (Komatsu et al. 2011).

We start by running large-scale simulations of a cosmological cube of side 40 Mpc, using 2×256^3 dark matter particles. This was done for two different models: a standard LCDM and a WDM model with a warm candidate of mass 2 keV produced in thermal equilibrium.

To compute the transfer function for WDM models, we used the fitting formula suggested by Bode et al. (2001):

$$T^2(k) = \frac{P^{\rm WDM}}{P^{\rm CDM}} = [1 + (\alpha k)^{2\nu}]^{-10/\nu}, \quad (2)$$

where α, the scale of the break, is a function of the WDM parameters, while the index ν is fixed. Viel et al. (2005) (see also Hansen et al. 2002), using a Boltzmann code simulation, found that $\nu = 1.12$ is the best fit for $k < 5\,h\,{\rm Mpc}^{-1}$, and they obtained the following expression for α:

$$\alpha = 0.049 \left(\frac{m_x}{1\,{\rm keV}}\right)^{-1.11} \left(\frac{\Omega_\nu}{0.25}\right)^{0.11} \left(\frac{h}{0.7}\right)^{1.22} h^{-1}\,{\rm Mpc}. \quad (3)$$

We used the expression given in equation (3) for the damping of the power spectrum for simplicity and generality. More accurate expressions for the damping of sterile neutrinos exist (e.g. Abazajian 2006) and show that the damping depends on the detailed physics of the early universe in a rather non-trivial way. The initial conditions for the two simulations have been created using the same random phases, in order to facilitate the comparison between the different realizations.

We then select one candidate halo with a mass similar to that of our Galaxy ($M \sim 10^{12}\,{\rm M}_\odot$) and resimulated it at higher resolution. These high-resolution runs are 8^3 times more resolved in mass than the initial ones: the dark matter particle mass is $m_p = 1.38 \times 10^5\,{\rm M}_\odot$, where each dark matter particle has a spline gravitation softening of 355 pc. This single halo has been resimulated in several different models; all simulations are summarized in Table 1 and three of the simulations are shown in Fig. 1.

Table 1. Simulation parameters.

Label	m_ν (keV)	$m_{\nu,\rm vel}$ (keV)	$v_0(z=0)$ (km s^{-1})	$N_{\rm vir}$ ($\times 10^6$)	$M_{\rm vir}$ ($\times\ 10^{12}\,{\rm M}_\odot$)
CDM	∞	–	–	10.2	1.42
WDM1	2.0	2.0	4.8×10^{-3}	8.6	1.22
WDM2	2.0	0.5	3.1×10^{-2}	8.4	1.20
WDM3	2.0	0.2	0.1	8.5	1.21
WDM4	2.0	0.1	0.26	6.7	0.93
WDM5	2.0	0.05	0.66	4.9	0.71

2.1 Streaming velocities

Particles that decouple whilst being relativistic are expected to retain a thermal velocity component. This velocity can be computed as a function of the WDM candidate mass (m_ν) according to the following expression (Bode et al. 2001):

$$\frac{v_0(z)}{1+z} = 0.012 \left(\frac{\Omega_\nu}{0.3}\right)^{1/3} \left(\frac{h}{0.65}\right)^{2/3} \left(\frac{1.5}{g_x}\right)^{1/3} \left(\frac{\rm keV}{m_\nu}\right)^{4/3} {\rm km\,s^{-1}}, \quad (4)$$

where z is the redshift. The distribution function is given by the Fermi–Dirac expression until the gravitational clustering begins (Bode et al. 2001).

This formalism is correct for the 'real' dark matter elementary particles (e.g. a sterile neutrino). In the N-body approach, we use macro particles (with masses of the order of $10^5\,{\rm M}_\odot$) to describe the density field. These macro particles effectively model a very large number of micro particles. Given that the velocities described in equation (4) have a random direction, the total velocity of the macro (N-body) particles should effectively be zero. Hence, it is not fully correct to directly use equation (4) to assign 'thermal' velocities to simulation particles.

On the other hand, the net effect of the thermal velocities is to create a finite upper limit in the phase-space distribution (PSD) due to their initial velocity dispersion (σ). What we are interested in is to recreate the same PSD limit in our simulation, and then study its effects on the dark matter halo density distribution. In order to achieve this goal, we proceed in the following way. From equation (4), we compute the rms velocity: $\sigma(z) = 3.571 v_0(z)$; we then create a Gaussian distribution centred on zero and with the same rms σ. Finally, we randomly generate particle velocities from this distribution and assign them to our macro particles. It is worth mentioning that the final results are almost independent of the assumed distribution for the velocities (Fermi–Dirac, Maxwellian, etc.), while they strongly depend on the strength of the velocity field (i.e. v_0).

In principle, adding random velocities introduces spurious momentum fluctuations into the initial conditions. For very light particles ($m_\nu \sim 1$ eV), this effect could be important and it could be balanced by introducing particles with opposite momenta (e.g. Gardini, Bonometto & Murante 1999). On the other hand, for the choices of WDM candidate masses in our paper, thermal velocities are quite modest ($\lesssim 0.5$ km s^{-1}) and lower than the Zeldovich ones. Hence, no artificial effects are expected.

As detailed in Section 3.1, there is a direct connection between m_ν and the expected size of the dark matter distribution core. This core is only due to the presence of thermal velocities and not, in the first approximation, to the cut in the power spectrum described by equation (2). Cutting the power spectrum changes the merger history of the dark matter halo but does not affect the density profile significantly (Moore et al. 1999). This implies that in order to study the effect of different values of m_ν (and hence v_0) it is sufficient to '*play*' with equation (4) leaving all other simulation parameters unaltered. Following this approach, we have generated several simulations using the same cut in the power spectrum (m_ν) but different initial thermal velocities ($m_{\nu,\rm vel}$), as detailed in Table 1.

3 RESULTS

Density profiles for the CDM run and the five WDM realizations (WDM1–5) are shown in Fig. 2. The profiles show a monotonic decrease of the central density as a function of the temperature of

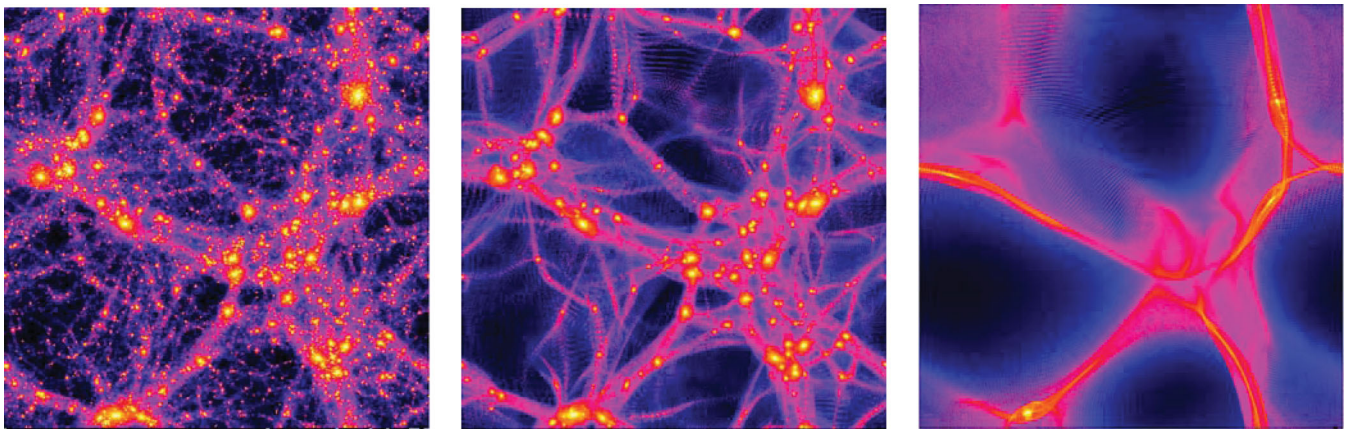

Figure 1. Density map of the large-scale (low-resolution) simulations ($L = 40$ Mpc) at redshift 0. From left to right: CDM, and two WDM with a cut in the power spectrum for a mass (m_ν) of 0.2 and 0.05 keV, respectively. The last two simulations have not been used in this paper and are presented only for illustration purposes, see Section 2.1 for more information.

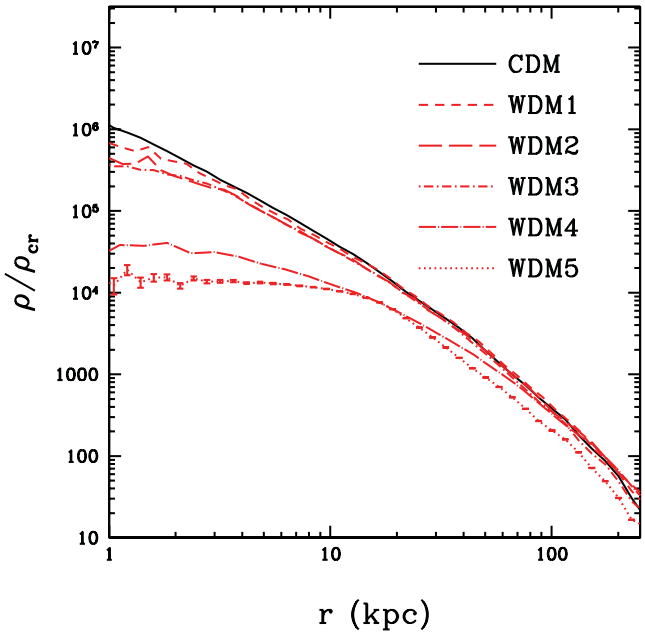

Figure 2. The spherically averaged density profiles for CDM, WDM1–5 haloes.

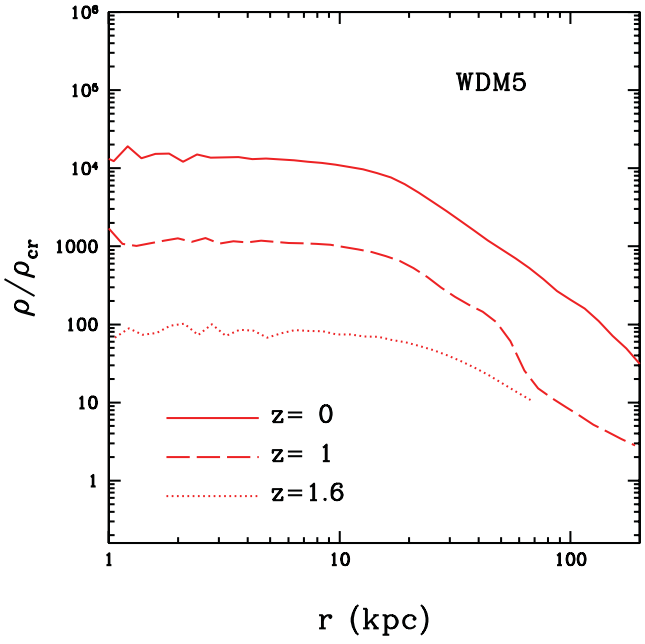

Figure 3. Time evolution of the density profiles for the WDM5 halo.

the dark matter candidate. Cold candidates show the usual cuspy behaviour (e.g. Dubinski & Carlberg 1991), while warmer candidates present a lower central density that becomes a clear core for $m_{\nu,\mathrm{vel}} = 0.05$ keV, with a size of several kpc.

Fig. 3 shows the time evolution of the density profile in the WDM5 simulation. The profile is already cored at a high redshift of $z = 1.6$, and the size of the core does not evolve substantially until $z = 0$. The profile only changes at large radii ($r > 50$ kpc) as a consequence of the assembly of the external part of the halo. This smooth mass accretion is also a consequence of the quiet merging history of the halo that does not undergo any merger with a mass ratio larger than 10 after $z = 2$. The assembly of the external part of the halo is consistent with a typical CDM halo in the outer regions.

As already mentioned, the theoretical explanation for the formation of a core is related to the presence of a maximum in the phase-space density distribution. This maximum is clearly visible in Fig. 4, where we plot the pseudo-phase-space density $Q \equiv \rho/\sigma^3$ for three different models, namely CDM, WDM3 and WDM5. For this latter model, the Q shows a large core that extends about 10 kpc. The WDM3 model also shows a strong flattening of the Q profile, consistent with a core distribution. On the other hand, the CDM pseudo-phase-space distribution is well fitted by a single power-law profile on the whole range, in agreement with previous results (Taylor & Navarro 2001; Schmidt, Hansen & Macciò 2008).

Fig. 5 shows the time evolution of the pseudo-PSD for our warmest candidate (i.e. thermal velocities for a 0.05-keV mass particle). The solid (blue) line shows the Q radial profile in the initial conditions ($z = 99$). This value has been calculated using only high-resolution particles that end up within 1.5 times the virial radius of the halo at $z = 0$. The other (red) lines represent the pseudo-PSD profile at different redshifts (from 1.6 to 0) and have been computed using all particles within the virial radius of the halo. All quantities in the plot are in physical units. The phase-space distribution shows very weak evolution with almost no evolution at all from $z = 99$ to 1.6. In the same plot, we also show the theoretical maximum

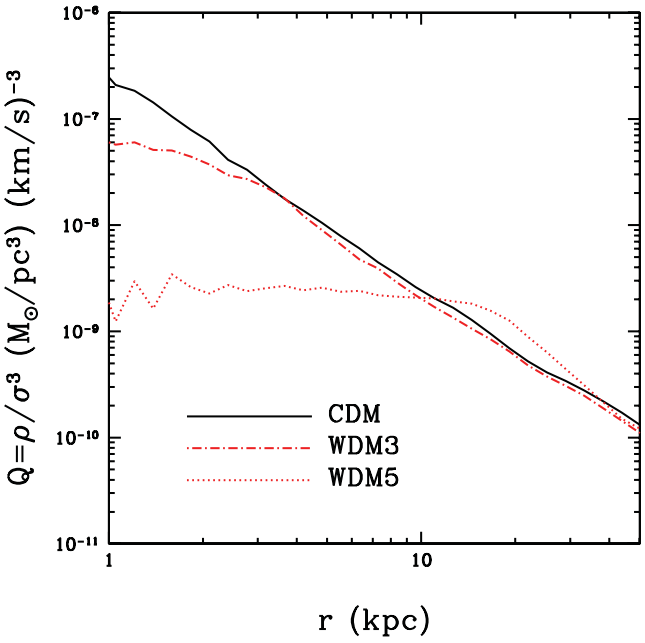

Figure 4. Phase-space density profile for the CDM, WDM3 and WDM5 models at $z = 0$.

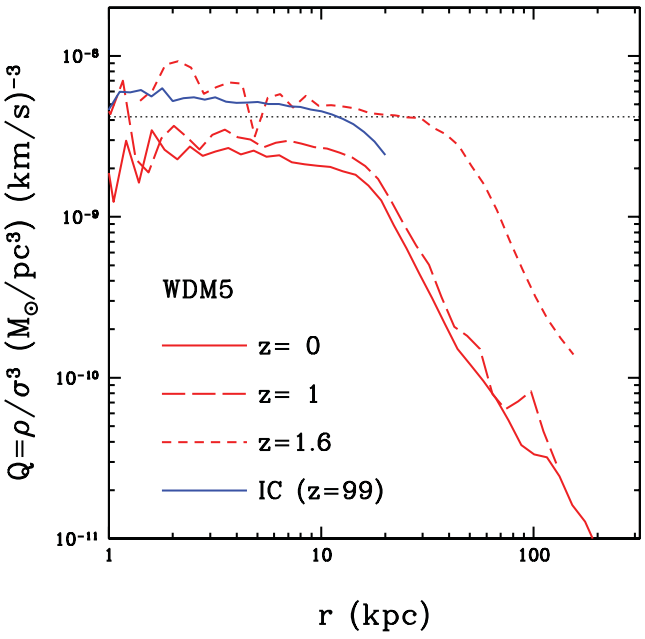

Figure 5. Time evolution of the pseudo-PSD radial profile for the WDM5 model. The black dotted line represents the theoretical prediction for the maximum value of Q according to equation (7).

phase-space density achievable by this model (see equation 7 for a rigorous definition of $Q_{\rm max}$).

The dotted (black) lines show predictions for $Q_{\rm max}$ for the *local* value of the matter density, which we measured directly from the simulation initial conditions using dark matter particles in the high-resolution region within a volume of $\approx$1 Mpc^3. The local density

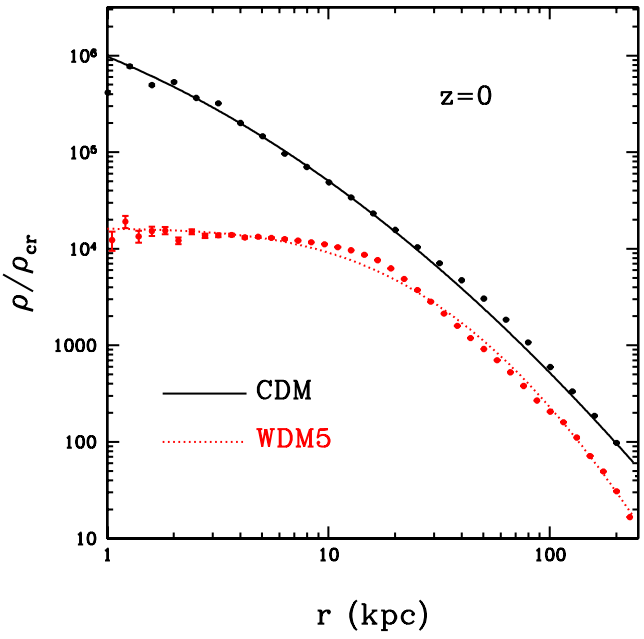

Figure 6. Density profiles for CDM and WDM5 and their fit using equation (5).

value turned out to be $\langle\rho\rangle_{\rm local} = 0.31\rho_{\rm cr}$.[4] The theoretical prediction is in quite good agreement with the simulation results.

In order to quantify the flatness (and the core size) of WDM profiles, we have fitted all our density profiles with the following parametric description, originally presented in Stadel et al. (2009):

$$\rho(r) = \rho_0 \exp(-\lambda[\ln(1 + r/R_\lambda)]^2). \quad (5)$$

In this parametrization, the density profile is linear down to a scale R_λ beyond which it approaches the central maximum density ρ_0 as $r \to 0$. We also note that if one makes a plot of d ln ρ/d ln $(1 + r/R_\lambda)$ versus ln $(1 + r/R_\lambda)$ then this profile forms an exact straight line with slope 2λ.

This fitting function is extremely flexible and makes possible to reproduce at the same time both cuspy profiles, like the one predicted by the CDM theory, and highly cored profiles, like in the WDM5 case (as shown in Fig. 6). The values of the parameter are obtained via a χ^2 minimization procedure using the Levenberg–Marquardt method. From now on, we will use the value of the fitting parameter R_λ as the fiducial value of the central density core in simulated profiles (hereafter $r_{\rm core,s}$). The $r_{\rm core,s}$ values for all our haloes are reported in the second column of Table 2.

3.1 Comparison with theoretical predictions

In Tremaine & Gunn (1979, hereafter TG79) limits on the mass of a neutrino are derived from the maximum phase-space density of a homogeneous neutrino background, with the further assumptions that neutrinos form bound structures and that their central regions can be well approximated by an isothermal sphere.

Assuming a Maxwellian velocity distribution, they obtained the maximum phase-space density:

$$Q_{\rm max} \equiv \frac{\rho}{\sigma^3} \propto m_\nu^4, \quad (6)$$

[4] This local value is slightly higher than the global one since it is computed around an object that will collapse and be fully virialized at $z = 0$.

Table 2. Size of density cores using different methods. See the text for a more detailed explanation.

Label	$r_{\rm core,s}$ (kpc)	$r_{\rm core,Q}$ (kpc)	$r_{\rm core,t}$ (kpc)
CDM	<0.4	<0.4	∞
WDM1	<0.4	<0.4	0.005
WDM2	<0.4	<0.4	0.075
WDM3	0.42	<1.1	0.48
WDM4	1.63	1.80	1.91
WDM5	4.56	4.85	6.98

where m_ν is the mass of the (warm) dark matter candidate. This limit has then been used in several follow-up papers to estimate the size of the density cores in WDM haloes (e.g. Dalcanton & Hogan 2001; Strigari et al. 2006).

Following TG79, we derive the theoretical expectation for the maximum pseudo-phase-space density and the size of the dark matter core for our WDM models adopting a slightly different approach. We can start from the definition of Q assuming to compute the density in some local volume L:

$$Q_{\rm max} \equiv \frac{\rho_L}{\sigma^3} = \frac{\frac{\rho_L}{\rho_{\rm cr}} \times \rho_{\rm cr}}{\sigma^3}, \quad (7)$$

where $\rho_{\rm cr} = 2.775 \times 10^{11}\, h^2\, {\rm M}_\odot\, {\rm Mpc}^{-3}$ is the critical density of the Universe and $\rho_L/\rho_{\rm cr}$ is the local density in our volume L, expressed in units of the critical density.

The denominator of equation (7) could be expressed as a function of the mass of the WDM candidate using equation (4) and the fact that for a Fermi–Dirac distribution the rms velocity is $\sigma = 3.571 v_0$. Combining equation (4) with equation (7), we get the following expression for $Q_{\rm max}$:

$$Q_{\rm max} = 1.64 \times 10^{-3} \left(\frac{\rho_L}{\rho_{\rm cr}}\right) \left(\frac{m_\nu}{\rm keV}\right)^4 \frac{{\rm M}_\odot\, {\rm pc}^{-3}}{\left({\rm km\, s}^{-1}\right)^3}, \quad (8)$$

where the numerical factor in front of the expression takes into account our choices for $\Omega_{\rm m}$ and h. This expression is formally equivalent to the one derived by TG79.

Finally, the maximum phase-space density can be converted in a 'core' size following Hogan & Dalcanton (2000):

$$r^2_{\rm core,t} = \frac{\sqrt{3}}{4\pi G Q_{\rm max}} \frac{1}{\left\langle \sigma^2_{\rm halo} \right\rangle^{1/2}}, \quad (9)$$

where $\sigma_{\rm halo}$ is the velocity dispersion (i.e. the mass) of the simulated dark matter halo. Values of $r_{\rm core,t}$ for our simulated haloes are reported in the last column of Table 2.

In the following, we will compare this theoretical value of the core ($r_{\rm core,t}$) with two different core sizes that can be estimated directly from the simulations. The first one is given by the R_λ parameter obtained by fitting the numerical density profile (as shown in Fig. 6) and we will refer to this value as $r_{\rm core,s}$. The second one is obtained by computing $Q_{\rm max}$ from the simulated density profile (as shown in Fig. 4) and then inserting this value in equation (9); we name this second parameter $r_{\rm core,Q}$.

Results for the three definitions of the core size for all our simulations are summarized in Table 2. Overall the three different estimators for the core size are in fairly good agreement. $r_{{\rm c},Q_{\rm max}}$ gives on average a larger value for the core, for the WDM4 and WDM5 runs, while for the WDM3 simulation it is only able to give an upper value, since there is not a clear indication of convergence towards a maximum value in the $Q_{\rm max}$ profile, as shown in Fig. 4.

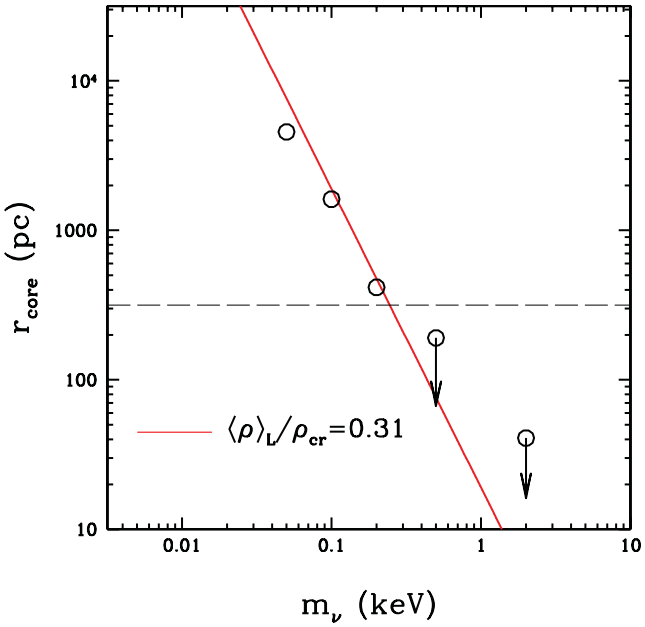

Figure 7. Comparison between core size in simulations (open symbols) and the theoretical expectation for an $M = 10^{12}\, {\rm M}_\odot$ halo (solid line). The dashed line is the gravitational softening of our simulations. All points below this line should be considered as upper limits on the core size.

Fig. 7 shows the comparison of the core found directly in simulations ($r_{\rm core,s}$, black symbols) with the core predicted by the above simple theoretical argument ($r_{\rm core,t}$). The solid line is obtained from equations (9) and (8), where, as discussed before, we used $\rho_L/\rho_{\rm cr} = 0.31$ as the value for the local density.

Overall numerical results for WDM3, WDM4 and WDM5 are in very good agreement with the theoretical expectations from equations (9) and (8). The WDM1 and WDM2 simulations only put upper limits on the size of the core, since the values of R_λ we obtain from fitting the density profile fall below the simulation softening (the dashed black line in the figure).

Using our determination of the core size as a function of the WDM mass, we compute the expected value of $r_{\rm core}$ for the typical halo mass ($5 \times 10^8\, {\rm M}_\odot$; see Macciò et al. 2010) of dwarf galaxies orbiting the MW. Results are shown in Fig. 8: the grey shaded area takes into account possible different values of the local matter density in the range $\rho/\rho_{\rm cr} = 0.15$–$0.6$.

From the figure it is clear that a core of $\approx$1 kpc would require a WDM mass of the order of 0.1 keV, well below current observational limits from large scales.

If we assume a WDM particle mass of $m_\nu \sim 2$ keV (represented by the dashed vertical line), in agreement with several astrophysical constraints (e.g. Viel et al. 2008), the maximum core size we can expect ranges from 10 pc for a massive, MW-like halo (see also Fig. 7) to 10–40 pc for a dwarf galaxy like halo. Finally, in predicting the core size for satellite galaxies in the MW halo, the fact that satellites can lose significant mass after accreting into larger haloes due to stripping and tidal forces must also be taken into account (e.g. Penarrubia, Navarro & McConnachie 2008; Macciò et al. 2010). This implies that the halo mass we may infer today for those galaxies is only a lower limit on the mass they had before accretion, which is the one to be used (as $\sigma^2_{\rm halo}$) in equation (9).

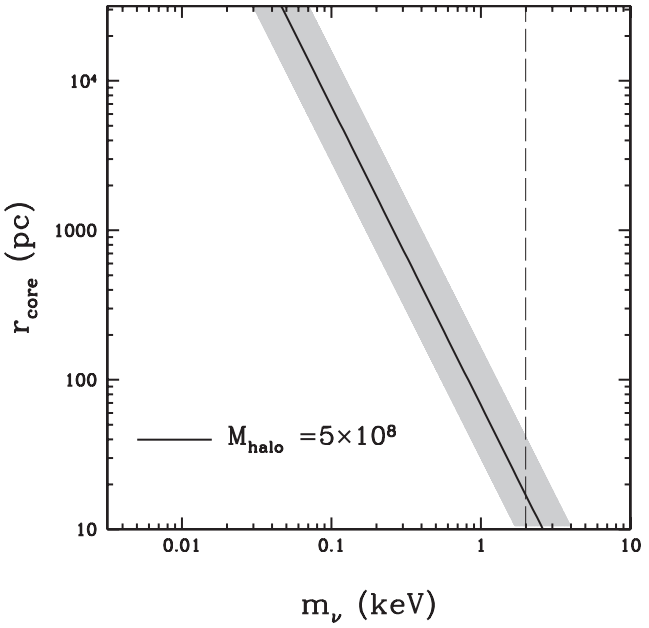

Figure 8. Expected core size for the typical dark matter mass of MW satellites as a function of the WDM mass m_ν. The shaded area takes into account possible different values of the local density parameter $0.15 < \Omega_m < 0.6$. The vertical dashed line shows the current limits on the WDM mass from large-scale structure observations.

4 CONCLUSIONS

We have used high-resolution *N*-body simulations to examine the effects of free-streaming velocities on halo internal structure in WDM models. We find the following.

(i) The finite initial fine-grained phase-space density (PSD) is also a maximum of the pseudo-PSD, resulting in PSD profiles of WDM haloes that are similar to CDM haloes in the outer regions; however, they flatten towards a constant value in the inner regions. This is in agreement with previous studies based on simulations (Colín et al. 2008) and theoretical arguments (Villaescusa-Navarro & Dalal 2011).

(ii) The finite PSD limit results in a constant density core with characteristic size that is in agreement with theoretical expectations, i.e. following TG79, especially if the value of the local matter density is taken into account.

(iii) The core size we expect for thermal candidates, allowed by independent constraints on large scales (Lyα and lensing, $m_\nu \approx 1$–2 keV), is of the order of 10–50 pc. This is not sufficient to explain the observed cores in dwarf galaxies that are nearly of kpc scale (Walker & Penarrubia 2011; Amorisco & Evans 2012; Jardel & Gebhard 2012).

(iv) Our results show that a core around kpc scale in dwarf galaxies would require a thermal candidate with a mass below 0.1 keV, a mass value ruled out by all large-scale structure constraints (Seljak et al. 2006; Miranda & Macciò 2007; Viel et al. 2008). Moreover, with such a warm candidate, the exponential cut-off of the power spectrum would make impossible to obtain these dwarf galaxies in the first place (e.g. Macciò & Fontanot 2010).

(v) Altogether these results lead to a nice 'Catch 22' problem for WDM: *if you want a large core you won't get the galaxy, if you get the galaxy it won't have a large core*.

We conclude that the solution of the cusp/core problem in Local Group galaxies cannot completely reside in simple models (thermal candidates) of WDM. If cores are required, then it seems that baryonic feedback (e.g. Romano-Díaz et al. 2008; Governato et al. 2010; Macciò et al. 2012a) is still the most likely way to alter the density profile of dark matter and hence reconcile observations with CDM/WDM predictions.

ACKNOWLEDGMENTS

We acknowledge stimulating discussions with George Lake, Jürg Diemand and Justin Read. We would like to thank A. Boyarsky, O. Ruchayskiy and S. Sergio Palomares-Ruiz for their help with the theory part of this work. Finally, we thank the referee of our paper, Adrian Jenkins, for several comments that improved the presentation and the clarity of our work. Numerical simulations were performed on the THEO and PanStarrs2 clusters of the Max-Planck-Institut für Astronomie at the Rechenzentrum in Garching and on the zBox3. SP would like to thank Joachim Stadel and Doug Potter for their crucial contribution to this project. AVM acknowledges funding by Sonderforschungsbereich SFB 881 'The Milky Way System' (subproject A1) of the German Research Foundation (DFG).

REFERENCES

Abazajian K., 2006, Phys. Rev. D, 73, 063506
Abazajian K., Koushiappas S. M., 2006, Phys. Rev. D, 74, 023527
Amorisco N. C., Evans N. W., 2012, MNRAS, 419, 184
Bertschinger E., 2001, ApJS, 137, 1
Bode P., Ostriker J. P., Turok N., 2001, ApJ, 556, 93
Bond J. R., Efstathiou G., Silk J., 1980, Phys. Rev. Lett., 45, 1980
Boyarsky A., Ruchayskiy O., Shaposhnikov M., 2009a, Annu. Rev. Nucl. Part. Sci., 59, 191
Boyarsky A., Lesgourgues J., Ruchayskiy O., Viel M., 2009b, J. Cosmol. Astropart. Phys., 5, 12
Boyarsky A., Ruchayskiy O., Iakubovskyi D., 2009c, J. Cosmol. Astropart. Phys., 3, 5
Boyarsky A., Lesgourgues J., Ruchayskiy O., Viel M., 2009d, Phys. Rev. Lett., 102, 201304
Buchmüller W., Covi L., Hamaguchi K., Ibarra A., Yanagida T., 2007, J. High Energy Phys., 3, 37
Colín P., Avila Reese V., Valenzuela O., 2000, ApJ, 542, 622
Colín P., Valenzuela O., Avila Reese V., 2008, ApJ, 673, 203
Dalcanton J. J., Hogan C. J., 2001, ApJ, 561, 35
de Blok W. J. G., McGaugh S. S., Bosma A., Rubin V. C., 2001, ApJ, 552, L23
de Vega H. J., Salucci P., Sanchez N. G., 2010, preprint (arXiv:1004.1908)
Diemand J., Zemp M., Moore B., Stadel J., Carollo M., 2005, MNRAS, 364, 665
Dodelson S., Widrow L. M., 1994, Phys. Rev. Lett., 72, 17
Dubinski J., Carlberg R. G., 1991, ApJ, 378, 496
Flores R. A., Primack J. R., 1994, ApJ, 427, L1
Gardini A., Bonometto S. A., Murante G., 1999, ApJ, 524, 510
Götz M., Sommer-Larsen J., 2002, Ap&SS, 281, 415
Governato F. et al., 2010, Nat, 463, 203
Hansen S. H., Lesgourgues J., Pastor S., Silk J., 2002, MNRAS, 333, 546
Hogan C. J., Dalcanton J. J., 2000, Phys. Rev. D, 62, 063511
Jardel J., Gebhardt K., 2012, ApJ, 746, 89
Khlopov M. Y., 2006, JETP Lett., 83, 1
Khlopov M. Y., Kouvaris C., 2008, Phys. Rev. D, 78, 065040
Klypin A., Kravtsov A. V., Valenzuela O., Prada F., 1999, ApJ, 522, 82
Knebe A., Devriendt J. E. G., Gibson B. K., Silk J., 2003, MNRAS, 345, 1285
Knebe A., Arnold B., Power C., Gibson B. K., 2008, MNRAS, 386, 1029
Komatsu E. (The WMAP Team) et al., 2011, ApJS, 192, 18

Kuzio de Naray R., Kaufmann T., 2011, MNRAS, 414, 3617
Kuzio de Naray R., McGaugh S. S., Mihos J. C., 2009, ApJ, 692, 1321
Macciò A. V., Fontanot F., 2010, MNRAS, 404, L16
Macciò A. V., Dutton A. A., van den Bosch F. C., Moore B., Potter D., Stadel J., 2007, MNRAS, 378, 55
Macciò A. V., Kang X., Fontanot F., Sommerville R. S., Koposov S. E., Monaco P., 2010, MNRAS, 402, 1995
Macciò A. V., Stinson G., Brook C. B., Wadsley J., Couchman H. M. P., Shen S., Gibson B. K., Quinn T., 2012a, ApJ, 744, L9
Macciò A. V., Ruchayskiy O., Boyarsky A., Munoz-Cuartas J. C., 2012b, preprint (arXiv:1202.2858)
Miranda M., Macciò A. V., 2007, MNRAS, 382, 1225
Moore B., 1994, Nat, 370, 629
Moore B., Ghigna S., Governato F., Lake G., Quinn T., Stadel J., Tozzi P., 1999, ApJ, 524, L19
Oh S.-H., de Blok W. J. G., Brinks E., Walter F., Kennicutt R. C., Jr, 2011, AJ, 141, 193
Pagels H., Primack J. R., 1982, Phys. Rev. Lett., 48, 223
Peebles P. J. E., Nusser A., 2010, Nat, 465, 565
Penarrubia J., Navarro J. F., McConnachie A. W., 2008, ApJ, 673, 226
Polisensky E., Ricotti M., 2011, Phys. Rev. D., 83, 043506
Romano-Díaz E., Shlosman I., Hoffman Y., Heller C., 2008, ApJ, 685, L105
Salucci P. et al., 2012, MNRAS, 420, 2034
Schmidt K. B., Hansen S. H., Macciò A. V., 2008, ApJ, 689, L33
Schneider A., Smith R. E., Macciò A. V., Moore B., 2011, preprint (arXiv:1112.0330)
Seljak U., Makarov A., McDonald P., Trac H., 2006, Phys. Rev. Lett., 97, 191303
Shi X., Fuller G. M., 1999, Phys. Rev. Lett., 82, 2832
Smith R. E., Markovic K., 2011, Phys. Rev. D, 84, 063507
Springel V. et al., 2008, MNRAS, 391, 1685
Stadel J., 2001, PhD thesis, Univ. Washington
Stadel J., Pooter D., Moore B., Diemand D., Madau P., Zemp M., Kuhlen M., Quilis V., 2009, MNRAS, 391, L21
Strigari L. E., Bullock J. S., Kaplinghat M., Kravtsov A. V., Gnedin O. Y., Abazajian K., Klypin A. A., 2006, ApJ, 652, 306
Takayama F., Yamaguchi M., 2000, Phys. Lett. B, 485, 388
Taylor J. E., Navarro J. F., 2001, ApJ, 563, 483
Tegmark M. (The SDSS Team) et al., 2006, Phys. Rev. D, 74, 123507
Tikhonov A. V., Gottlöber S., Yepes G., Hoffman Y., 2009, MNRAS, 399, 1611
Tremaine S., Gunn J. E., 1979, Phys. Rev. Lett., 42, 407 (TG79)
Viel M., Lesgourgues J., Haehnelt M. G., Matarrese S., Riotto A., 2005, Phys. Rev. D, 71, 063534
Viel M., Becker G. D., Bolton J. S., Haehnelt M. G., Rauch M., Sargent W. L. W., 2008, Phys. Rev. Lett., 100, 041304
Villaescusa-Navarro F., Dalal N., 2011, J. Cosmol. Astropart. Phys., 1103, 024
Waler M. G., Penarrubia J., 2011, ApJ, 742, 20
Wang J., White S. D. M., 2007, MNRAS, 380, 93
Zavala J., Jing Y. P., Faltenbacher A., Yepes G., Hoffman Y., Gottlöber S., Catinella B., 2009, ApJ, 700, 1779
Zentner A. R., Bullock J. S., 2003, ApJ, 598, 49

This paper has been typeset from a TEX/LATEX file prepared by the author.